PHYSICAL PROPERTIES OF SOME ANTARCTIC METEORITES

Kiyoshi YOMOGIDA and Takafumi MATSUI

Geophysical Institute, Faculty of Science, University of Tokyo, Yayoi 2-chome, Bunkyo-ku, Tokyo 113

Abstract: The intrinsic and bulk densities, porosities and ultrasonic-wave velocities (V_p and V_s) in three mutually perpendicular directions were measured in five antarctic meteorites (ordinary chondrites; ALH-77288, -77294, -78103, -78251 and MET-78003). V_p and V_s measurements were made at the room temperature and under one atmospheric pressure. Measured V_p and V_s values are fairly smaller than those expected from their mineral compositions except for ALH-77288. High porosity values ($\sim 10\%$) of the samples, except for that ($\sim 2\%$) of ALH-77288, are consistent with such low elastic-wave velocities. Degree of decrease in velocity is, however, larger than that expected from spherical pores. Thus, V_p and V_s of chondrites may be controlled by the crack porosity. Very low transmitting efficiency of the shear-wave may also support this view. Velocity anisotropy between transmitting directions is observed in almost all samples. The thermal diffusivity of four antarctic meteorites (ordinary chondrites; ALH-769, -77231, Y-74191 and -74371) was measured under the vacuum condition (below 10^{-3} mmHg) in the temperature range of 100 to 500 K. Thermal diffusivities of chondrites are also smaller than those expected from their mineral compositions and are ascribed to their high porosity values. The thermal diffusivities at 300 K are $2.7 \sim 5.0 \times 10^{-7}$ m^2/s. The thermal diffusivity of ALH-77231 was measured for three mutually perpendicular directions. However, significant difference of thermal diffusivity between directions was not detected. We cannot find a correlation between the measured physical quantities and the petrologic types so far.

1. Introduction

Systematic measurements of the physical properties of chondrites are important for revealing the nature of their parent bodies and their origin. However, reported data (ALEXEYEVA, 1958, 1960; MATSUI and OSAKO, 1979; MATSUI *et al.*, 1980) have been few so far except for magnetic properties. We have a good opportunity to measure the physical properties systematically on a number of meteorites that have been collected in Antarctica since 1969.

We have already reported some data on the physical properties of several antarctic meteorites (MATSUI and OSAKO, 1979; MATSUI *et al.*, 1980). In this paper we present the results of the physical property measurements of the samples recently distributed to us. Although the number of samples is still not great enough to derive any definite generalizations on the nature of the chondrites, several interesting features

are noticed.

2. Sample Descriptions

For the elastic constants the five antarctic meteorites are measured in this study: ALH-77288, -77294, -78103, -78251 and MET-78003. And for the thermal diffusivity the four meteorites are measured: ALH-769, -77231, Y-74191 and -74371. Most antarctic meteorites usually suffered heavy weathering and so they often have large cracks and weathering rust. Therefore, we selected carefully the fresh samples with no weathering rust and apparent large cracks since such features are clearly due to the secondary effects. The measured values are thus considered to represent a characteristic nature of each sample.

Table 1. Intrinsic and bulk densities and porosity.

Sample	Type	Volume	Mass	Density (g/cm^3)		Porosity
		(cm^3)	(g)	Bulk	Intrinsic	(%)
ALH-77288	H6	4.55	13.65	3.69	3.77	2.0
ALH-77294	H5	2.91	9.76	3.35	3.84	12.9
ALH-78103	L6	4.47	14.46	3.23	3.73	13.4
ALH-78251	L6	4.55	14.64	3.22	3.70	13.2
MET-78003	L6	2.61	8.69	3.33	3.61	7.8

Although simple petrographic observations of the five samples for the elastic property measurements have been already reported by MASON (1981), we have checked the petrographic characteristics of our samples. The classification of the samples given by MASON (1981) is shown in Table 1. The following are the descriptions of the petrographic characteristics of our samples by NAGAHARA (private communication, 1981).

ALH-77288

The section consists mainly of olivine with minor amounts of orthopyroxene and plagioclase. Many metal or troilite grains can be also seen. Low-Ca pyroxene is orthorhombic and high-Ca clinopyroxene cannot be observed. Plagioclase is well-crystallized and is as large as 100 μm. The relics of shock effects are not observed. Chondrules are sparse but there are some relics of radial, barred and porphyritic chondrules. The matrix is strongly recrystallized and turns to be large crystals. Glassy parts have changed to an assembly of fine grains. Limonitic staining is very small.

ALH-77294

The section shows well-developed chondritic structure and consists mainly of

olivine and pyroxene. Neither plagioclase, high Ca clinopyroxene nor glass can be seen. There exist both clino- and orthopyroxene in the low-Ca pyroxene and the former shows polysynthetic twins. Various types of chondrules are set in the matrix composed of cryptocrystalline materials. There is no black opaque matrix. Nickel-iron metal and troilite are present around the chondrules but there is only a little limonitic staining around them.

ALH-78103

The section consists mainly of olivine with minor amounts of clino- and orthopyroxene. There is abundant well-crystallized secondary plagioclase. Chondrules are sparse and have quite diffuse margins. It is barely possible to identify the relic texture of chondrules such as barred and radial ones. Groundmass in chondrules and matrix are strongly recrystallized and turn to be an assembly of fine crystals (mostly of olivine). A large amount of limonitic staining is present around nickel-iron grains.

ALH-78251

The section consists mainly of olivine and orthopyroxene with minor amounts of clinopyroxene and plagioclase. The degree of crystallization of plagioclase is not as high as that of other minerals. A large crystalline plagioclase looks turbid or consists of an assembly of small grains. Neither the outline nor the structure of chondrules can be defined but there is quite a little relic texture of barred and glassy chondrules. The recrystallized parts and the relics are almost all holocrystalline. Limonitic staining is prominent around the nickel-iron grains.

MET-78003

The section consists mainly of olivine and pyroxene (ortho- and high-Ca clinopyroxene) with minor amounts of large well-crystallized plagioclase. The outline of chondrules almost vanishes but it is possible to identify the structure such as radial, barred, glassy and porphyritic. Groundmass in chondrules and matrix turn to be an assembly of fine grains. Minor limonitic staining is associated with the nickel-iron grains.

3. Experimental Techniques

The intrinsic density, ρ_0, was measured by using the helium-pycnometer (the model 1302 Helium-Air Pycnometer, Shimadzu Seisakusho Ltd). Accuracy of the measurement is very much dependent on an amount of the sample and a temperature of the ambient atmosphere. Specifically, a slight variation of the ambient temperature affects significantly the measurements. Thus, the measured ρ_0 values are scattered a little bit. The diversity of the ρ_0 data is, however, within 2% as shown in Fig. 1. The bulk density, ρ_{bulk}, was simply calculated from the mass and the volume

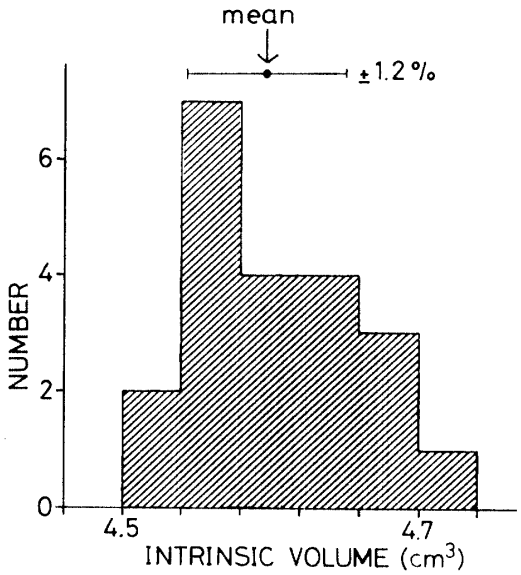

Fig. 1. An example of diversity of the intrinsic density measurements (ALH-77288).

of the sample. By cutting and grinding the samples, we prepared the sample into a precisely rectangular shape. Therefore, the volume of the sample is measured with an accuracy less than 1%. The porosity, ϕ, is calculated from $\phi = 1 - \rho_{bulk}/\rho_0$.

Ultrasonic-wave velocity was measured by employing the pulse transmission method under one atmospheric pressure and at the room temperature condition. Velocity measurements were conducted for three mutually perpendicular directions. 1 MHz PZTs were used. No detectable changes in velocity values accompanying the difference in the frequency of transducers can be seen. For the V_p measurement, the onset of the signal was clear and thus the accuracy of V_p determination is better than a few %. We could successfully measure the shear-wave velocity, V_s, for the relatively low porosity samples (ALH-77288, -77294 and MET-78003). Because of the scattering effect of cracks and pores, the onset point of *S*-wave was very difficult to determine accurately for the sample with higher porosity. In Fig. 2 we show two examples of the received signal: one is an example for a clear onset (ALH-77288) and the other is for a blurred one (ALH-78103). Accuracy of V_s determination was thus nearly 10% except for the case of ALH-77288. V_s values of the two samples, ALH-78103 and -78251, cannot be measured due to their higher porosity than those of the previous samples. Although we can determine the onset point even for the unsuccessful case, it shifted significantly with the subtle change of measuring conditions such as pulse width, pulse height, contact state between the sample and the transducers, and so on.

Thermal diffusivity was measured by the modified Angstrom method in vacuum below 10^{-3} mmHg and the temperature range of 100 to 500 K.

The reader may refer to MATSUI and OSAKO (1979) and MATSUI *et al.* (1980) for further details of the experimental techniques mentioned above.

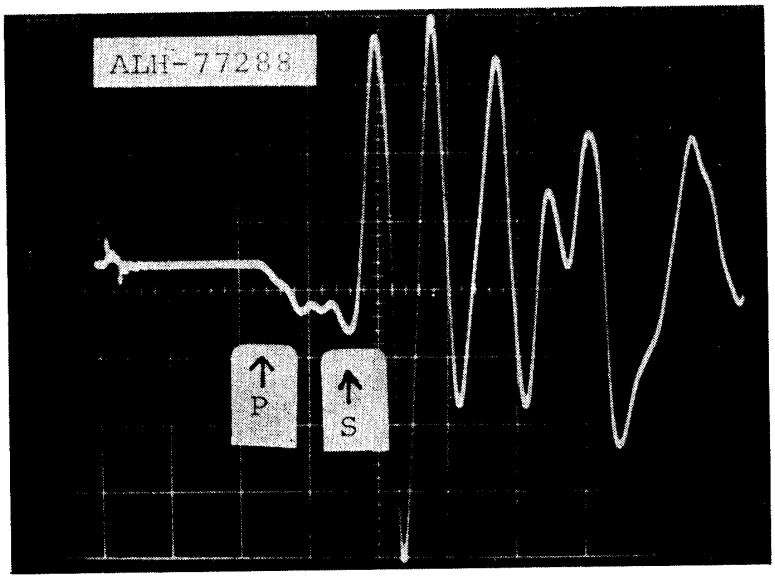

Fig. 2a. An example of a clear onset of the received S-wave (ALH-77288).

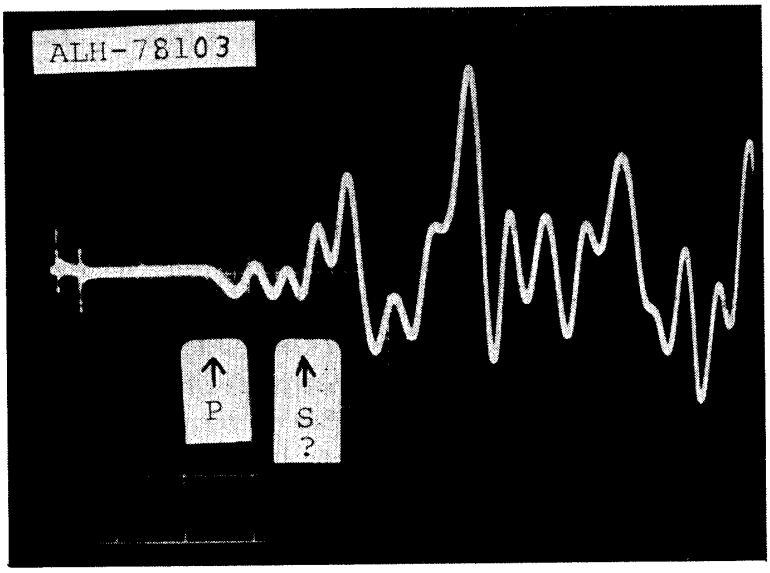

Fig. 2b. An example of a blurred onset of the received S-wave (ALH-78103).

4. Results and Discussion

4.1. Density and porosity

The intrinsic and bulk densities and porosities of the five samples are summarized in Table 1. A very low porosity of ALH-77288 is noticed. The porosity of ALH-77288 is the lowest of all the samples that we have ever measured. It is also noticed that the porosities of L6 chondrites significantly differ from each other. The intrinsic

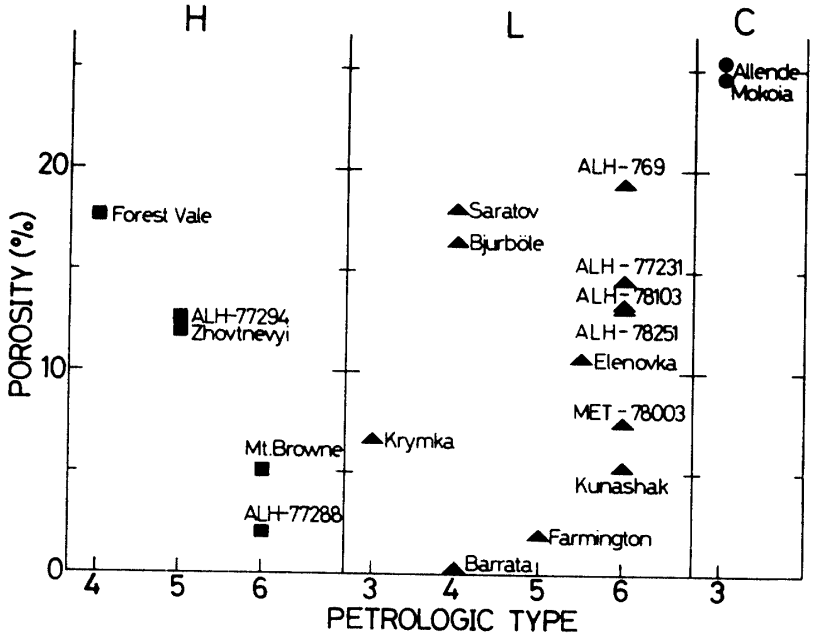

Fig. 3. Porosity versus petrologic-type systematics of each chondrite group.

densities of the H chondrites are shown to be larger than those of the L chondrites because of the higher nickel-iron metal content of the H chondrites. All the available porosity data of chondrites (ALEXEYEVA, 1958; STACEY *et al.*, 1961; MATSUI *et al.*, 1980) are plotted against the respective petrologic type in Fig. 3. If the degree of the consolidation increases with the maximum temperature which the chondrites have experienced, that is, the sintering temperature, the porosity is expected to decrease with the petrologic type (YOMOGIDA and MATSUI, 1981) and might be a good measure of a consolidation of composite materials of chondrites. The porosity of the H chondrites appears to be correlated with the petrologic type. On the other hand, no such correlation can be observed for the L chondrites. Scattered porosity values of the L6 chondrites may suggest that the secondary effects such as the thermal and/or shock crackings have disturbed the original consolidated state for the L6 chondrites. In any event, it is tentatively concluded that we cannot see any correlation between the porosity and the petrologic type for the L chondrites. It is necessary to aquire more data for unequilibrated chondrites (type 3 or 4) in order to reach a definite conclusion on the above problem. The difference between the L and H chondrites is very interesting if the tendency observed here is true, because the amount of metal may play a key role in the solidification process of ordinary chondrites.

4.2. Elastic-wave velocity

The results of the ultrasonic-wave velocity measurements are summarized in Table 2. V_p and V_s of chondrites are much smaller than those expected from the

mineral composition of chondrites except for ALH-77288. The compressional-wave velocity versus porosity are plotted in Fig. 4. As known from this figure, low elastic-wave velocity of chondrites is ascribed to the high porosity of chondrites. However,

Table 2. Elastic-wave velocity.

Sample	Direction	Length (mm)	Velocity V_p (km/s)	Velocity V_s (km/s)
ALH-77288	L1	14.85	6.96	3.92
	L2	15.63	7.07	3.88
	L3	15.92	6.62	3.73
ALH-77294	L1	13.73	2.58	1.58
	L2	13.73	2.68	1.49
	L3	15.46	2.72	—
ALH-78103	L1	14.76	2.36	—
	L2	16.52	2.30	—
	L3	18.34	2.21	—
ALH-78251	L1	15.08	2.30	—
	L2	17.27	2.40	—
	L3	17.48	2.40	—
MET-78003	L1	13.00	4.48	2.01
	L2	13.21	4.71	1.93
	L3	15.20	4.85	2.45

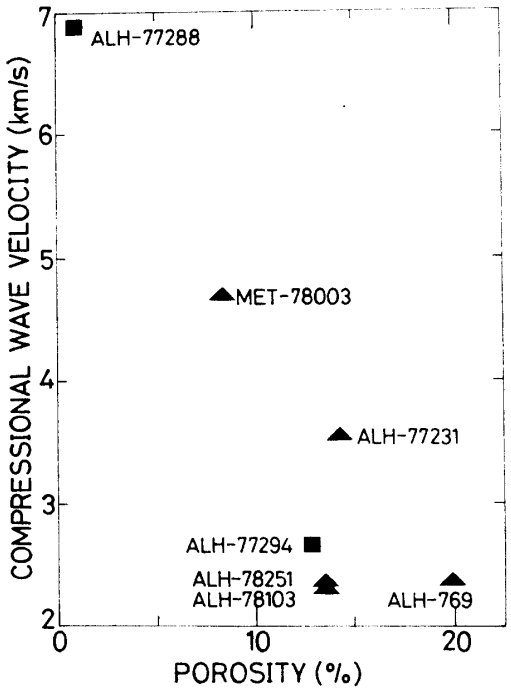

Fig. 4. Mean compressional-wave velocity versus petrologic-type systematics. ▲ and ■ represent L and H chondrites, respectively.

degree of decrease in velocity ($\sim$70% for $\phi=\sim$10%) is much larger than that calculated from the spherical pores ($\sim$6% decrease in velocity due to spherical pores for $\phi=\sim$10%). The velocity versus porosity relation may suggest that the low velocity is due to the high crack porosity of these samples. The extraordinary high velocity of ALH-77288 is noticed. The V_p of ALH-77288 is even higher than that of pure iron (5.92 km/s; MOLOTOVA and VASSIL'EV, 1960) but is fairly smaller than that of either pure single crystalline olivine (8.42 km/s for $Fo_{93}Fa_7$; KUMAZAWA and ANDERSON, 1969) or pyroxene (7.78 km/s for $En_{80}Fs_{20}$; FRISILLO and BARSCH, 1972).

As shown in Table 2, there exists the velocity anisotropy between transmitting directions for some samples. The velocity decreases with the sample length for ALH-78103. Such a tendency might be explained by the scattering effect due to the existence of many pores. However, we have not observed such a tendency for the other samples. On the contrary, we can see a reversed tendency in some samples. The velocity anisotropy for the low porosity samples such as ALH-77288 and MET-78003 may suggest that the oriented distribution of microcracks causes such anisotropy besides contribution of the anisotropy of crack shapes. If this interpretation is the case, we may be able to get some information on internal structures of the chondritic parent bodies from detailed analysis of the velocity anisotropy.

The isotropic elastic constants of chondritic samples are calculated from the observed V_p, V_s and ρ_{bulk}. In Table 3 the calculated elastic constants are summarized.

Table 3. Elastic properties of stony meteorites.

Sample	Type	ρ_{bulk} (g/cm^3)	ρ_0 (g/cm^3)	ϕ (%)	V_p (km/s)	V_s (km/s)	λ (kbar)	μ (kbar)	K (kbar)	E (kbar)	ν
ALH-77288	H6	3.69	3.77	2.0	6.89	3.84	663	544	1026	1387	0.27
ALH-77294	H5	3.35	3.84	12.9	2.66	1.54	78.1	79.4	131	195	0.25
ALH-78103	L6	3.23	3.73	13.4	2.29	—	—	—	—	—	—
ALH-78251	L6	3.22	3.70	13.2	2.36	—	—	—	—	—	—
MET-78003	L6	3.33	3.61	7.8	4.68	2.13	427	151	528	1170	0.37

4.3. Thermal diffusivity

We have measured the thermal diffusivity of four samples. The description of the samples is given in Table 4. All the samples have rectangular shapes except for ALH-769. For ALH-769 owing to its fragile nature we cannot prepare the sample into a precisely rectangular shape. The thermal diffusivity of Yamato-74191 and -74371 has already been measured in the temperature range of 300 to 550 K by MATSUI and OSAKO (1979). In this study we measured the thermal diffusivity of these samples in the temperature range of 100 to 300 K.

Results are shown in Fig. 5. The thermal diffusivity shows a fairly large temperature dependency. The data were fitted to the empirical formula, $k=A+B/T$

Table 4. Sample description for thermal diffusivity measurements.

Sample	Type	Size (mm)	Mass (g)	Bulk density (g/cm³)
ALH-769	L6	3.14×3.51×3.79	0.121	—
ALH-77231	L6	3.71×3.88×3.96	0.183	3.2
Y-74191	L3	4.16×2.89×3.31	0.125	3.1
Y-74371	H5–6	3.48×2.71×3.58	0.112	3.3

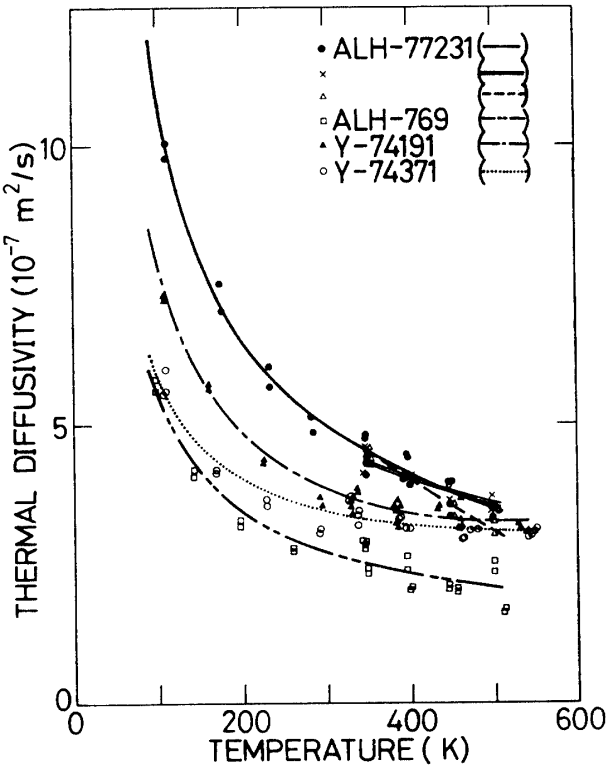

Fig. 5. Thermal diffusivity, k, versus temperature, T, for ALH-769, -77231, Y-74191 and -74371.

$+CT^3$ (FUJII and OSAKO, 1973), to obtain smoothed values, where k is the thermal diffusivity and T is the absolute temperature. Coefficients were determined by the least-squares fitting and are tabulated in Table 5. The smoothed diffusivity values are tabulated in Table 6 and shown in Fig. 5. For ALH-77231 we measured the thermal diffusivities for three mutually perpendicular directions between 300 to 500 K. However, significant anisotropy of the thermal diffusivity between three directions is not detected. The small thermal diffusivity values of ALH-769 may be due to its high porosity and are almost similar to those of the lunar breccia (MIZUTANI and OSAKO, 1974). We cannot find any correlation between the thermal diffusivity and

Table 5. Coefficients A, B and C of the empirical equation for thermal diffusivity ($k=A+B/T+CT^3$).

Sample	A (10^{-7} m^2s^{-1})	B (10^{-4} $m^2s^{-1}K$)	C (10^{-15} $m^2s^{-1}K^{-3}$)
ALH-769	1.38±0.22	0.406±0.034	−0.118±0.183
ALH-77231			
(3.71)	2.27±2.66	0.899±0.814	−0.793±0.878
(3.88)	1.41±3.31	1.01 ±1.01	0.119±1.10
(3.96)	2.17±0.22	0.872±0.037	−0.383±0.175
Y-74191	1.76±0.14	0.597±0.245	0.186±0.101
Y-74371	2.14±0.15	0.362±0.242	0.174±0.105

Table 6. Thermal diffusivity, k (10^{-7} m^2s^{-1}), of antarctic meteorites.

Temperature (K)	Sample					
	ALH-769	ALH-77231* L1	L2	L3	Y-74191	Y-74371
100	5.44			10.9	7.74	5.76
150	4.09			7.97	5.75	4.56
200	3.40			6.50	4.76	3.97
250	2.99			5.60	4.18	3.62
300	2.70	5.05	4.82	4.97	3.80	3.40
350	2.49	4.50	4.36	4.50	3.55	3.25
400	2.32	4.01	4.02	4.10	3.37	3.16
450	2.18	3.55	3.77	3.76	3.26	3.10
500	2.05	3.08	3.59	3.43	3.19	3.08

* L1=3.71 mm, L2=3.88 mm, L3=3.96 mm.

the petrologic type.

5. Summary

The results of the present study are summarized as follows:

i) The intrinsic densities of the H chondrites are larger than those of the L chondrites, which may reflect the difference in nickel-iron metal content.

ii) The porosity of the L chondrites shows no correlation to the petrologic type. However, the porosity of the H chondrites seems to show a correlation to the petrologic type.

iii) The ultrasonic-wave velocities of chondrites are dependent on the crack porosity.

iv) The velocity anisotropy between transmitting directions is observed for

some samples up to a degree of $\sim 10\%$. It might be ascribed to either the anisotropy of crack shapes or the oriented distributions of microcracks, or both.

v) The thermal diffusivity of chondrites is very much dependent on the porosity values and has no correlation to the petrologic type.

Acknowledgments

The authors express their sincere thanks to Prof. T. NAGATA for his permission to use the meteorite samples throughout the course of this work, to Ms. Y. NAGAHARA for the petrographic description of the thin sections of the samples we received, and to Mr. K. KURITA for technical advice in measuring the elastic-wave velocity. The authors also would like to thank Prof. M. KUMAZAWA for his critical comments which have improved the manuscript.

References

ALEXEYEVA, K. N. (1958): Physical properties of stony meteorites and their interpretation based on the hypothesis on the origin of meteorites. Meteoritika, **16**, 67–77.

ALEXEYEVA, K. N. (1960): New data on physical properties of stony meteorites. Meteoritika, **18**, 68–76.

FRISILLO, A. L. and BARSCH, G. R. (1972): Measurement of single-crystal elastic constants of bronzite as a function of pressure and temperature. J. Geophys. Res., **77**, 6360–6384.

FUJII, N. and OSAKO, M. (1973): Thermal diffusivity of lunar rocks under atmospheric and vacuum conditions. Earth Planet. Sci. Lett., **18**, 65–71.

KUMAZAWA, M. and ANDERSON, O. L. (1969): Elastic moduli, pressure derivatives, and temperature derivatives of single-crystal olivine and single-crystal forsterite. J. Geophys. Res., **74**, 5961–5972.

MASON, B. (1981): Antarctic Meteorite Descriptions 1976–1977–1978–1979, ed. by R. SCORE *et al.* Antarct. Meteorite Newsl., **4**(1).

MATSUI, T. and OSAKO, M. (1979): Thermal property measurement of Yamato meteorites. Mem. Natl Inst. Polar Res., Spec. Issue, **15**, 243–252.

MATSUI, T., HAMANO, Y. and HONDA, M. (1980): Porosity and compressional-wave velocity measurement of antarctic meteorites. Mem. Natl Inst. Polar Res., Spec. Issue, **17**, 268–275.

MIZUTANI, H. and OSAKO, M. (1974): Elastic-wave velocities and thermal diffusivities of Apollo 17 rocks and their geophysical implications. Proc. Lunar Sci. Conf. 5th, 2891–2901.

MOLOTOVA, L. V. and VASSIL'EV, YU. I. (1960): Velocity ratio of longitudinal and transverse waves in rocks, II. Izv. Acad. Sci, USSR, Phys. Solid Earth, **8**, 731–743.

STACEY, F. D., LOVERING, J. F. and PARRAY, L. G. (1961): Thermomagnetic properties, natural magnetic moments, and magnetic anisotropies of some chondritic meteorites. J. Geophys. Res., **66**, 1523–1534.

YOMOGIDA, K. and MATSUI, T. (1981): Porosity of ordinary chondrite—Is it a good measure of a consolidation state of composite materials of chondrite?—. Lunar and Planetary Science XII. Houston, Lunar Planet. Inst., 1227–1229.

(Received May 16, 1981; Revised manuscript received August 7, 1981)